Environmental Science and Pollution Research (2021) 28:53578–53593
https://doi.org/10.1007/s11356-021-14570-6

RESEARCH ARTICLE

Effect of nanoparticle on rheological properties of surfactant-based nanofluid for effective carbon utilization: capturing and storage prospects

Ravi Shankar Kumar[1] · Rishiraj Goswami[2] · Krishna Raghav Chaturvedi[1] · Tushar Sharma[1]

Received: 18 January 2021 / Accepted: 20 May 2021 / Published online: 25 May 2021

Abstract

Previous studies have shown insufficient dispersion and thermal stability of nanofluids for high-temperature carbon capture and storage applications. Compared to the other NPs, TiO_2 nanofluids exhibit superior stability due to their high zeta potential. In previous studies, TiO_2 nanofluids have shown superior performance in heat transfer and cooling applications along with importing the stability of other nanofluids like SiO_2 in form of nanocomposites. Therefore, in this study, a nanofluid formulation consisting of titania nanofluid in a base solution of ethylene glycol (EG) with different co-stabilizers such as surfactants was synthesized for better dispersion stability, enhanced electrical, and rheological properties especially for the use in high-temperature industrial applications which include carbon capture and storage along with enhanced oil recovery. The formulated nanofluid was investigated for stability using dynamic light scattering (DLS) study and electrical conductivity. Additionally, the formulated nanofluid was also examined for thermal stability at high temperatures using an electrical conductivity study followed by rheological measurements at 30 and 90 °C. At a high temperature, the shear-thinning behavior of EG was found highly affected by shear rate; however, this deformation was controlled using TiO_2 nanoparticles (NPs). Furthermore, the role of surfactant was also investigated on dispersion stability, electrical conductivity followed by viscosity results, and it was found that the nanofluid is superior in presence of anionic surfactant sodium dodecyl sulfate (SDS) as compared to nonionic surfactant Triton X-100 (TX-100). The inclusion of ionic surfactant provides a charged layer of micelles surrounding the core of a NP and it produced additional surface potential. Consequently, it increases the repulsive force between two adjacent NPs and renders a greater stability to nanofluid while nonionic surfactant allowed monomers to adsorb on the surface of NP via hydrophobic interaction and enhances the short-range interparticle repulsion, to stabilize nanofluid. This makes titania nanofluid suitable for widespread high-temperature applications where conventional nanofluids face limitations. Finally, the application of the synthesized titania nanofluids was explored for the capture and transport of CO_2 where the inclusion of the anionic surfactant was found to increase the CO_2 capturing ability of titania nanofluids by 140–220% (over the conventional nanofluid) while also showing superior retention at both investigated temperatures. Thus, the study promotes the role of novel surfactant-treated titania nanofluids for carbon removal and storage and recommends their applications involving carbonated fluid injection (CFI) to carbon utilization in oilfield applications.

Keywords Carbon capture · Electrical conductivity · Nanofluid · Rheology · Temperature · Titania

Introduction

The increase in atmospheric carbon, which has been emitted due to growing industrialization and rising economic growth, has caused runaway climate change, global warming, and threatens human survival (Leung et al. 2014; Asadi-Sangachini et al. 2019; Al Mesfer 2020). Hence, carbon capture and storage has attracted considerable research interest in the recent past, with the government and policymakers also recognizing the important role of carbon capture in meeting

Responsible Editor: Tito Roberto Cadaval Jr

✉ Tushar Sharma
tusharsharma.ism@gmail.com

[1] Enhanced Oil Recovery Laboratory, Department of Petroleum Engineering, Rajiv Gandhi Institute of Petroleum Technology, Amethi, Jais, UP 229304, India

[2] Oil India Limited, Duliajan, Assam 786602, India

climate change guidelines (Schrag 2007). The main impetus in the development of carbon capture technology has focused on the development of new methods for CO_2 removal from the exhaust of thermal coal-fired power plants, which are among of the highest emitters of CO_2 from a single-point source (Jain et al. 2013; Azzolina et al. 2016; Pilorgé et al. 2020). Recent research activity has thus focused on the development of high-efficiency and less energy-intensive processes for reducing the carbon footprint of power plants to achieve net-zero carbon emissions (Jiang et al. 2019). This can be achieved by capturing the CO_2 from the flue gas released by the burning of hydrocarbons and this process is known as post-combustion capture of CO_2. Thus, the development of chemicals with improved absorption kinetics, stability, and thermodynamics for post-combustion capture of CO_2 has attracted considerable research interest and funding (Liu et al. 2019). Commonly used chemicals for CO_2 capture are monoethanolamine (MEA), methyl diethanolamine (MDEA), triethylenetetramine (TETA), ionic liquids, and deep eutectic solvents (DES) which have been found to have high CO_2 absorption loading and low energy consumption (Haider et al. 2018; Borhani and Wang 2019; Krishnan et al. 2020). However, their application is impacted by oxidative (which occurs in the presence of O_2) and thermal degradation (Vega et al. 2014). The loss of efficiency resulting from the thermal degradation of conventional absorbents is highly challenging. Furthermore, ongoing research work is focused on exploring solvents which not only exhibit superior CO_2 capturing but are also injectable in subsurface reservoirs, thereby ensuring effective carbon geo storage (Leung et al. 2014). Thus, there is a need to explore new chemicals for the effective removal of carbon at high temperatures without compromising CO_2 capturing ability.

Recent developments in the domain of colloidal solutions have demonstrated their extensive applicability in several industrial applications including oilfield operations due to their intrinsic properties such as stability, viscosity contrast, and electrical nature (Saidur et al. 2011). Nanofluids have shown potential applications in heat transfer (Al-Waeli et al. 2019), cooling (Tiwari et al. 2013), refrigeration (Ding et al. 2009), biomedical (Lam et al. 2014), and other carbon storage applications such as drilling and well completion (Rafati et al. 2018), cementing (Thakkar et al. 2019), and fossil fuel mobilization applications (Wei et al. 2016; Yuan and Wang 2018). In previous studies, nanofluids have demonstrated superior CO_2 loading for carbon capture applications (Peyravi et al. 2015; Zhang et al. 2018; Rezakazemi et al. 2019). However, the nanofluid characteristics and stability play an important role in any of their practical applications (Ahmed et al. 2018). Therefore, a detailed study of their rheological properties and stability parameters becomes imperative. Similar to other chemical absorbents, it is a well-highlighted fact that nanofluids and their formulations exhibit degradation with temperature. At high temperatures, nanofluids lose their stability and viscoelastic properties rendering them inefficient. Thus, stabilizing the fluid system is extremely crucial for high-temperature applications. Huminic and Huminic (2012) reviewed the application of nanofluids in heat exchangers and concluded that the thermo-physical properties and flow inside the exchanger mainly depend upon the efficiency of nanofluids. In addition to this, the nanofluids used in industrial applications are not always stationary; thus, the analysis of rheological properties becomes important to determine their dynamic nature and efficacy for practical applications.

In a previous study, Chaturvedi and Sharma (2020) compared the CO_2 absorption and oil mobilization potential of SiO_2, ZnO, and TiO_2 nanofluids prepared in a base fluid of 1000 ppm PAM who found that while CO_2 underwent physical absorption in both SiO_2 and TiO_2 nanofluids, it underwent chemical trapping (chemisorption) in ZnO nanofluids which was also observed in a separate study (Haghtalab et al. 2015). Separately, the CO_2 absorption performance in a tray column of SiO_2 and Al_2O_3 enhanced MeOH-based absorbents was compared and SiO_2 was found to perform better in this role (Torres Pineda et al. 2012). Similarly, the application of Al_2O_3, SiO_2, Fe_3O_4, and CNT nanofluids (base fluid: distilled water) was investigated for CO_2 removal using a gas-liquid. Various nanofluid formulations exhibit different dispersion and rheological properties at varying temperatures, thus laying greater importance on their screening process for different applications. For example, TiO_2-based nanofluid exhibits higher stability than SiO_2 nanofluid as was reported in our previous study (Kumar and Sharma 2018, 2020). Additionally, the concentration of nanoparticles (NPs) is also a limiting factor and may vary from application to application. Thus, TiO_2 has proven to be the most promising NPs which has high dispersion stability and rheological properties but its application in the oilfield is limited by an upper limit of 0.1 wt% due to subsurface pore-trapping and blockage concerns (Esfandyari Bayat et al. 2014). On the other hand, a higher concentration of TiO_2 is recommended for heat transfer or cooling applications (Demir et al. 2011). The conventional oilfield polymers like polyacrylamide (PAM), hydrolyzed polyacrylamide (HPAM), polyvinyl alcohol (PVA), and natural polymers like xanthan gum have been used in the preparation of nanofluids due to their superior rheological and particle stabilizing behavior for various thermal, mass transfer, and flow applications (William et al. 2014; Chaturvedi et al. 2020). Peyghambarzadeh et al. (2011) explored water-ethylene glycol (EG)–based nanofluids for coolant applications in car radiators and reported that the heat transfer properties have a high dependency on NPs concentration. Previous studies have explored the use of various nanofluids for the physical absorption of CO_2. Zare et al. (2019) studied the effect of water-based nanofluid of TiO_2 and found around a 60% increase in adsorption efficiency in water-based nanofluid (when compared to distilled water). In a separate study, Jiang et al. (2014) also confirmed the higher order of adsorption capacity of CO_2 using TiO_2 NPs which they attributed to the higher adsorption capacity of TiO_2 when compared to other NPs such as MgO, Al_2O_3, and SiO_2. A similar effect was also confirmed by Wang et al. (2016) that TiO_2 nanofluids of

Table 1 A comprehensive literature study showing the use of nanofluid (NPs and polymer) at elevated temperature for different applications

Authors	Base fluid	NP	Concentration	Temperature (°C)	Study
Chen et al. (2007)	EG	TiO_2	≤ 1.8 vol.%	20–40	Rheology and thermal conductivity
Xie et al. (2010)	EG	MgO	5 vol.%	10–60	Rheology and thermal conductivity
		Al_2O_3	5 vol.%		
		TiO_2	5 vol.%		
		ZnO	5 vol.%		
		SiO_2	5 vol.%		
Palabiyik et al. (2011)	PG	Al_2O_3	1–9 vol.%	20–80	Dispersion stability and thermal conductivity
		TiO_2	1–9 vol.%		
Satti et al. (2017)	PG-W (60:40)	Al_2O_3	0.5–6 vol.%	− 30 to 90	Thermal conductivity
		TiO_2	0.5–6 vol.%		
		ZnO	0.5–6 vol.%		
		SiO_2	6 vol.%		
		CuO	0.5–1.5 vol.%		
Kumar and Sharma (2018)	PAM	SiO_2	0.5 wt%	25–90	Dispersion stability, electrical conductivity, and rheology
		TiO_2	0.5 wt%		
		$SiO_2 + TiO_2$	0.5 wt% + 0.05–0.1 wt%		
Kumar et al. (2020)	HPAM	SiO_2	0.1–1.0 wt%	25–90	Thermal stability, rheology, and oil recovery
		TiO_2	0.1 wt%		
		$SiO_2 + TiO_2$	0.1–1.0 wt% + 0.1 wt%		

monoethanolamine (MEA) showed maximum CO_2 absorption among other NPs such as SiO_2 and Al_2O_3. Separately, nanofluids have also been used to transport CO_2 as feedstock for methane recovery from natural gas hydrate reservoirs (Nashed et al. 2018). In addition to this, the selection of EG-based titania nanofluid was done due to the inherent properties of both EG and TiO_2. The first advantage of taking EG as a base fluid is its applicability over a wide temperature range, and similar observations have been reported by several researchers in numerous industrial applications (Sekrani and Poncet 2018). Moreover, the use of TiO_2 is safer due to less negative effects found on exposure in previous studies as compared to other nanomaterials and it can be easily obtained due to its large industrial-scale production (Grassian et al. 2007). On the other hand, the titania NPs stability is higher as compared to the other NPs and also holds high thermal efficiency which makes it feasible for high-temperature industrial application with EG. Compared to a water-based nanofluid, ethylene glycol was used as the suspension fluid of the nanofluid because the stated objective of preparing the nanofluid was its used for CO_2 absorption at high temperature. While water has a boiling point of 100 °C, ethylene glycol has a boiling point of 197 °C. In general, the uniform distribution of NPs exhibit higher dispersion stability, which help to maintain sustainable rheological properties and, as a result, can curtail the effect of temperature (Peyghambarzadeh et al. 2011). However, electrical conductivity studies and rheological analysis for EG-based titania nanofluid at elevated temperatures are not widely available in the literature. Therefore, a proper experimental study depicting the temperature effect on nanofluid stability, concentration, and rheological behaviour can be of great interest for several industrial applications including oilfield. In addition to this, the novelty of the current work lies in the surfactant role on NP stability and surfactant-treated nanofluids to be proposed for CO_2 capture from flue gases at the higher temperature.

Following a comprehensive literature study (Table 1), it was observed that there is a distinct lack of literature available for CO_2 absorption using nanofluids at high temperatures (i.e., 75–90 °C). Hence, the CO_2 absorption was explored at a high temperature which is more commonly encountered in the flue stacks of coal-fired power plants. In nanofluids, surfactants are generally utilized to enhance the dispersion stability of NPs within the nanofluid. The inclusion of SDS as anionic surfactant provides an additional charged layer around the individual NPs and produce a uniform distribution of NPs via strong electrostatic repulsion in between the particles renders greater stability to nanofluid, while TX-100 as a nonionic surfactant allowed monomers to get adsorbed on the surface of NP via hydrophobic interaction and enhances the short-range interparticle repulsion, to stabilize nanofluid. In addition, the CO_2 capturing ability would be higher after the inclusion of surfactant (Chaturvedi et al. 2021). Therefore, this study confirms two major attributes over the issues of conventional nanofluid used for CO_2 capture which are (1) inclusion of surfactant reduces the agglomeration of NPs and provides uniform distribution of NP within the nanofluids and (2) the uniformly distributed NPs enhance the CO_2 capturing ability via showing maximum interaction with CO_2 molecules.

Thus, in this study, we have focused on stability analysis and rheological properties of EG-based TiO_2 (0.05–1.0 wt%) nanofluid. However, it is very clear that the NPs form agglomerates which deteriorate their rheological behavior. Thus, anionic sodium dodecyl sulfate (SDS) and nonionic Triton X-100 (TX-100) are utilized as co-stabilizer to enhance the dispersion stability of nanofluid which may have a favorable impact on the rheological properties of nanofluid. Finally, the CO_2 absorption potential of the various nanofluids was explored using the pressure decay method. The formulated nanofluid may show higher potential for several industrial

Table 2 Compositional details of formulated fluids/nanofluids and nomenclature

Base fluid	TiO_2 (wt%)	Surfactant	Nomenclature	Remark
Ethylene glycol (EG)	--	--	EG	EG
	0.05		ET-0.05	ET
	0.10		ET-0.1	
	0.50		ET-0.5	
	1.00		ET-1.0	
	--	SDS (0.15 wt%)	EGS	EGS
	0.05		ETS-0.05	ETS
	0.10		ETS-0.1	
	0.50		ETS-0.5	
	1.00		ETS-1.0	
	--	TX-100 (0.02 wt%)	EGT	EGT
	0.05		ETT-0.05	ETT
	0.10		ETT-0.1	
	0.50		ETT-0.5	
	1.00		ETT-1.0	

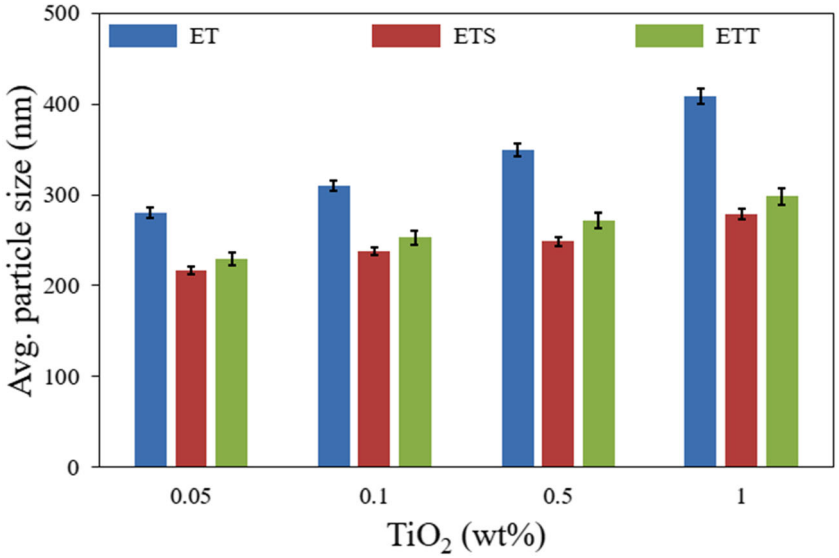

Fig. 1 Size distribution details of titania nanofluid with and without surfactant SDS and TX-100

applications including carbon capture and storage where conventional fluids face limitations at elevated temperature.

Materials and methods

Materials and equipment used in this study

For this study, ethylene glycol (EG), of molecular weight 62.07 g/mol, was obtained from the MERCK group, India, and used as received. The hydrophilic and rutile TiO_2 NPs (purity 99.00%, size ~ 20 nm, specific surface area ~ 50 m^2/g) were used as obtained from Sisco Research Laboratories (SRL)Pvt. Ltd, India. Surfactants, sodium dodecyl sulfate (SDS) (anionic, purity > 99.5%) was used as received from Sisco Research Lab Pvt. Ltd. India. Nonionic surfactant triton X-100 of density 1.06 g/ml (purity ~ 99.00%; molecular weight ~ 646.87 g/mol) was used as received from Thomas Baker, India. The detailed composition of the prepared nanofluids and their nomenclature used throughout the study are given in Table 2.

Preparation of nanofluid

In this study, the TiO_2 nanofluid was synthesized in a base fluid of EG and proposed for high-temperature industrial applications including oilfield. The nanofluid was prepared in the base solution of EG by the inclusion of TiO_2NPs in a varying concentration ranging from 0.05 to 1.0 wt%. Both the base fluid and TiO_2 NPs in required wt% were mixed properly using a Mixer (USHA, India) of varying speed (5000–15,000 rpm) was used to synthesize the titania nanofluid. After that, a laboratory-grade magnetic stirrer was used to mix the surfactant in the formulated nanofluid (see Table 2). After that, anionic surfactant SDS at critical micelle concentration (CMC ~ 0.15 wt%) was mixed properly using a magnetic stirrer for half an hour and formed a bulk group of nanofluid ETS. Similarly, nonionic surfactant (CMC ~ 0.02 wt%) was also mixed in the nanofluid and form a group ETT.

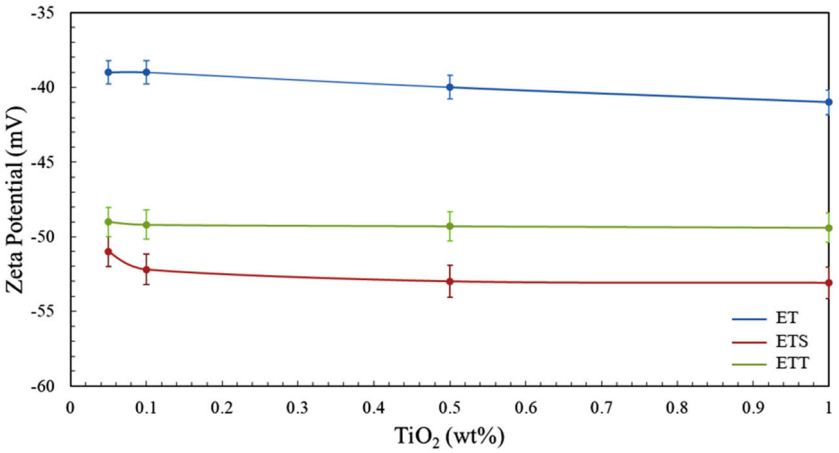

Fig. 2 Zeta potential result of nanofluid stabilized by anionic (SDS) and nonionic (TX-100) surfactant at ambient condition

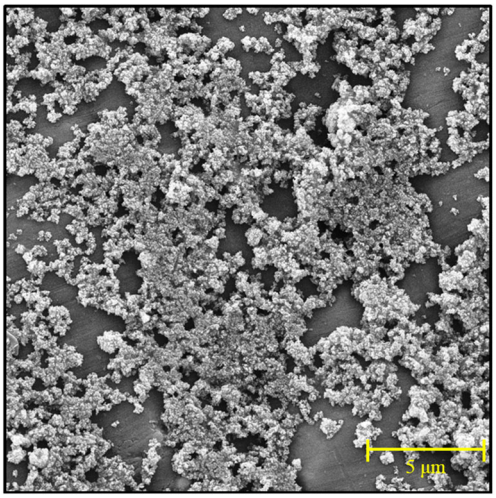

Fig. 3 Appearance of TiO_2 nanofluid under field emission scanning electron microscopy (FESEM) showing agglomeration and clusters of large size

The CMC values of both the surfactant were determined using the stalagmometric method and confirmed using the electrical conductivity method as it was adopted in our previous study (Kumar et al. 2020; Chaturvedi and Sharma 2021). Generally, at CMC, surfactant forms micelles in the nanofluid which ensures uniform distribution of NPs within the nanofluid. The method adopted to prepare the titania nanofluid is similar to one of our previous studies (Kumar and Sharma 2018, 2020). Finally, nanofluids after preparations were sonicated for 1 h using a digital ultrasonic cleaner (LMUC2A, Labman India) of frequency 40 ± 3 kHz at an ultrasonic voltage 50 W were used to sonicate nanofluids at a desirable frequency to ensure uniform distribution of NPs within the nanofluid. The compositional detail and nomenclature of all the formulated nanofluids used in this study are provided in Table 2.

Characterization of TiO_2 nanofluid

The formulated nanofluids were characterized for size and zeta potential using Zetasizer (NanoZS, Malvern® France) working on the principle of dynamic light scattering (DLS) to analyze the colloidal stability. The measurements of zeta potential and average particle size were investigated at ambient conditions. The cuvette/cell was properly cleaned in each experiment and dried using a hot air dryer to avoid contamination within the samples. The refractive index (RI) and adsorption index (AI) of the used material were 1.336 and 0.700, respectively. Field emission scanning electron microscopy (FESEM) was used to analyze the surface morphology of formulated EG-based nanofluid. An instrument called Nova NanoSEM was utilized for this purpose. The formulated nanofluid samples were collected on a 1 cm^2 microscopic glass slide and dried in an oven at 100 °C for 3 days to remove the liquid content from the formulated nanofluid. The microscopic glass slide containing dried nanofluid samples were gold coated before FESEM analysis. The electrical conductivity of nanofluid is necessary for various industrial applications. The electrical conductivity ensures the uniform dispersion of NPs within the nanofluid wherein any

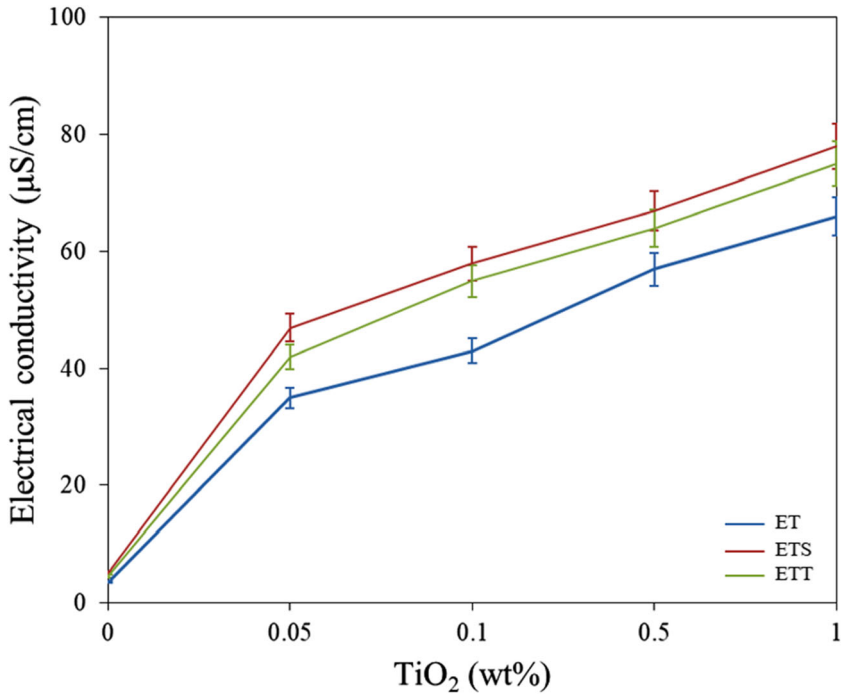

Fig. 4 Electrical conductivity of ethylene glycol, formulated nanofluids, and role of surfactant on electrical conductivity at ambient condition

physical changes in the nanofluid may disturb the nanofluid electrical conductivity at elevated temperatures. Thus, NPs' physical stability was determined using an electrical conductivity meter (Model: HI98129, Hanna Instruments® USA) at varying temperatures (30–90 °C). Finally, viscosity analysis as a part of the rheological study for nanofluid samples was performed using an HPHT rheometer (MCR-52, Anton Paar, Austria). The rheometer parts consisting of bob and the cup were properly cleaned during each measurement. A varying shear rate was applied ranging from 1 to 1000 s^{-1}. The viscosity measurements were performed at ambient temperature and high temperature (30–90 °C) to see the thermal degradation of nanofluids.

CO_2 absorption study in nanofluids

The CO_2 absorption study in the nanofluids was performed using a high pressure-high temperature stirring pot with pressure and temperature transducers. The CO_2 capturing apparatus used in this study is similar to one of our previous studies (Chaturvedi et al. 2018). The internal volume of the stirring pot was 100 ml and it was mounted on a stainless steel stand. An impeller suspended at the end of a shaft driven by the electric motor was used to provide the required agitation to the nanofluid during CO_2 absorption. The method for CO_2 absorption was the pressure decay method (Tolesorkhi et al. 2018). Initially, a nanofluid of desired volume (35–50 ml) is put inside the stirring pot and following that, it is vacuumed to remove any residual gases. Then, CO_2 (or any other gas) is introduced into the stirring pot at the required pressure, and the drop in its pressure is continuously recorded. Finally, after some time, no further fall in pressure would take place, which denotes that no further CO_2 absorption is now possible. For this study, high purity (99.95%) CO_2 and (99%) N_2 gas were used.

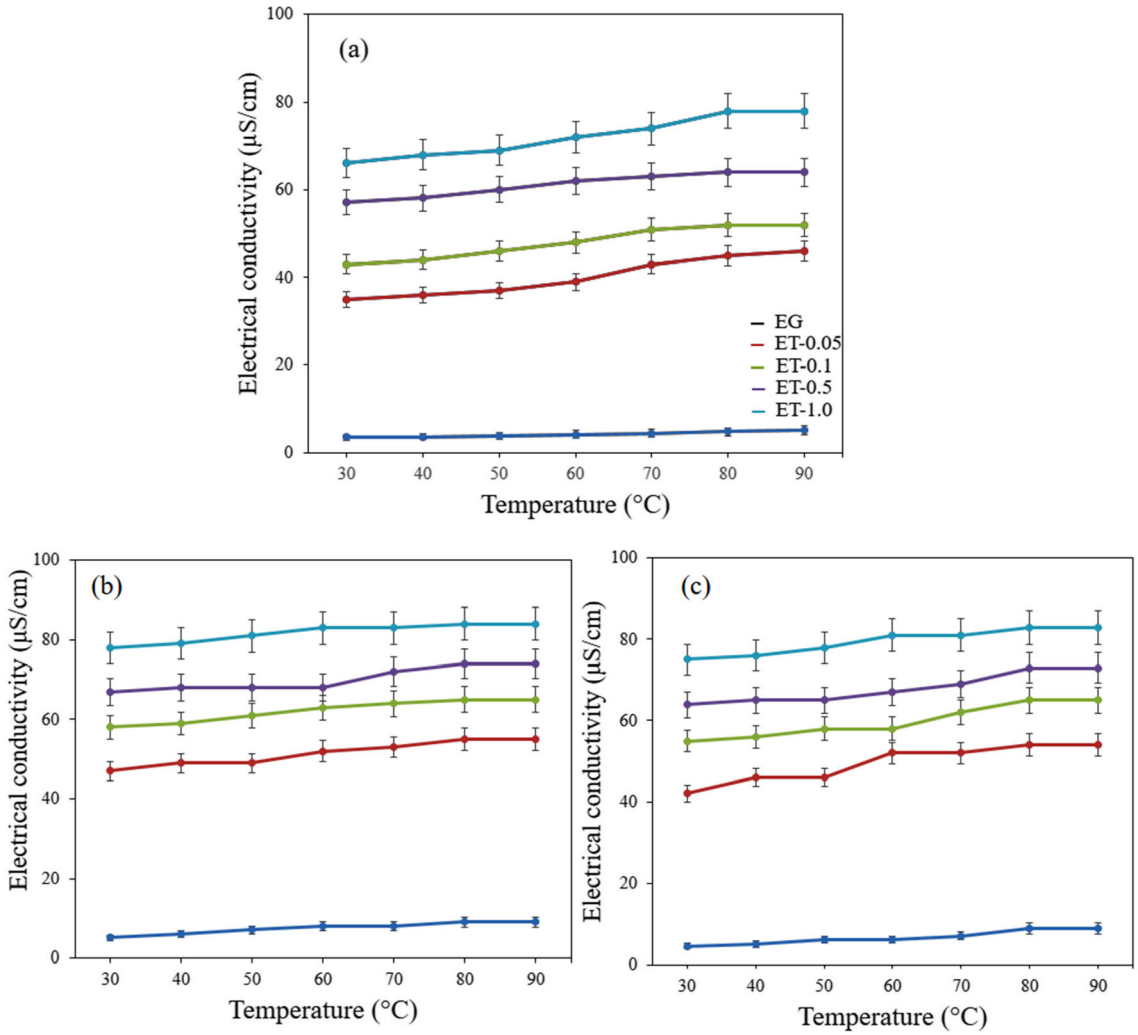

Fig. 5 Result showing electrical conductivity with varying temperature (30–90 °C): **a** EG, EG-titania nanofluids, **b** with anionic surfactant SDS, **c** nonionic surfactant TX-100

Results and discussion

Stability of nanofluid

Size distribution and zeta potential measurement are an important method to explore nanofluid stability, in which the size of the NPs within the formulated nanofluids can be analyzed and further the zeta potential of the NPs suspension can be measured (Haddad et al. 2014; Jiang et al. 2016). The size of TiO_2 NPs used in this study was ~ 20 nm; however, the size distribution results showed a significant increase in size that indicates the agglomeration tendency of TiO_2 NPs due to attractive forces between the homogeneous NPs within the nanofluid. The average particle size for ET nanofluid was determined 280, 310, 350, and 409 nm for ET-0.05, ET-0.1, ET-0.5, and ET-1.0, respectively, and shown in Figs. 1 and 2. Now, from this study, it is clear that NPs tend to agglomerate and form large clusters (see Fig. 3 of FESEM) that are not recommended for industrial applications due to several reasons such as flow line blockage and sedimentation in the flow line. In oilfield operations, this agglomeration may hamper the oil recovery by blocking of pores in porous media and limit the efficacy of nanofluid in subsurface applications. However, it was observed that this agglomeration of NPs can be controlled using other stabilizing agents such as surfactants (Al-Anssari et al. 2017). Subsequently, size reduction was observed after the inclusion of SDS and TX-100 surfactants in the nanofluid. In general, the surfactant forms micelles on the surface of NPs which helped to maintain uniform distribution within the nanofluid. The obtained average of the size was 217, 238, 249, and 279 nm for ETS-0.05, ETS-0.1, ETS-0.5, and ETS-1.0, respectively after the addition of anionic surfactant SDS. Similarly, the size was determined 229, 253, 272, and 298 nm for ETT-0.05, ETT-0.1, ETT-0.5, and ETT-1.0, respectively after the addition of TX-100. The reason for the reduction in the size of NPs within the nanofluid is attributed to the inclusion of surfactants along with polymers. Generally, polymer-based nanofluid provides resistance to the NPs to agglomeration and sedimentation by maintaining viscosity contrast in the nanofluid network as compared to conventional water-based nanofluid (Kumar and Sharma, 2018). However, surfactants improve the surface charge of the NPs and the overall repulsive forces acting between the similar charged NPs increase that can be measured by zeta potential measurement of DLS study (Al-Anssari et al. 2017). Also, it was observed that the size of NPs increases with an increase in the NP concentration due to the increased population of TiO_2 NPs which leads to their more random movement and collisions within the nanofluid, causing further agglomeration and sedimentation (Nashed et al. 2018).

The zeta potential measurement generally states the stability of nanofluid; if the measured value obtained is higher than ± 30 mV, the nanofluid is said to be stable (Setia et al. 2013). In this study, the zeta potential results showed higher values and it was determined − 39, − 39.2, − 40, and − 41 mV for ET-0.05, ET-0.1, ET-0.5, and ET-1.0, respectively and are shown in Fig. 2. In addition to this, the zeta potential values increase with the inclusion of surfactants in the nanofluid. Thus, the zeta potential was obtained − 51, − 52.2, − 53, and − 53.4 mV for ETS-0.05, ETS-0.1, ETS-0.5, and ETS-1.0, respectively after the addition of anionic surfactant SDS. The anionic surfactant generally forms micelles via adsorption on NP surfaces and increases the net surface charge of NPs which are in suspension (Kumar et al. 2020). The increase in surface charge enhances the interparticle distance within the nanofluid thusly increases the repulsive forces between the NPs within the nanofluid and makes the nanofluid stable via uniform dispersion. Similarly, the zeta potential was determined − 49, − 49.2, − 49.5, and 50.1 mV for ETT-0.05, ETT-0.1, ETT-0.5, and ETT-1.0, respectively after addition of TX-100. The surfactant TX-100 holds a neutral charge; it helped to enhance the surface potential of nanofluid via lying of micelles on the NPs surface which forms a protective layer and reduces the attractive forces acting between the NPs in nanofluid; thus, the uniform distribution of NPs remains maintained via reduced agglomeration. Now, this study confirms that nanofluid stability can be improved via the inclusion of surfactant which

Table 3 Electrical conductivity results at 80–90 °C

Temperature (°C)	Electrical conductivity (μS/cm)				
	EG	ET-0.05	ET-0.1	ET-0.5	ET-1
80	4.8	45	52	64	78
82	4.8	45	52	64	78
84	4.8	45	52	64	78
86	5.1	46	52	64	78
88	5.1	46	52	64	78
90	5.22	47	52	64	78
Temperature (°C)	Electrical conductivity (μS/cm)				
	EGS	ETS-0.05	ETS-0.1	ETS-0.5	ETS-1.0
80	9	55	65	74	84
82	9	55	65	74	84
84	9	55	65	74	84
86	9	55	65	75	85
88	9	55	65	75	85
90	9	55	65	75	85
Temperature (°C)	Electrical conductivity (μS/cm)				
	EGT	ETT-0.05	ETT-0.1	ETT-0.5	ETT-1
80	8.8	54	65	73	83
82	8.8	54	65	73	83
84	8.8	54	65	73	83
86	8.8	54	65	73	83
88	9	54	65	74	84
90	9	54	65	74	84

not only improves the zeta potential but also reduces the agglomeration of NPs and provide support to maintain uniform distribution of NPs within the nanofluid and make nanofluid stable. In addition, zeta potential results of DLS study clearly shows the zeta potential value of formulated nanofluids is greater than ± 30 mV which is in the range of stable category (Setia et al. 2013) which provided good credibility for stable rheological properties, which are key to nanofluids holding high efficacy in flow applications.

FESEM analysis

The morphology of titania NPs within EG-based nanofluid (ET-0.5) was imagined using FESEM and is shown in Fig. 3. The image of dried TiO_2 nanofluid shown in Fig. 3 was captured at an acceleration voltage of 10 kV. The individual size TiO_2 NPs used in this study was 20 nm; it is clear that NPs agglomerate during nanofluid preparation. Therefore, large-sized clusters can be seen in Fig. 3, consistent with the size distribution results of DLS analysis in the "Stability of nanofluid" section. In addition, from the FESEM study, it can be observed that nanofluid exhibited agglomeration which led to the formation of large clusters which were several magnitudes in size larger than the sole NPs (of reported size ≈ 20 nm) (Fig. 3).

Electrical conductivity measurements

The electrical conductivity of nanofluid is a good representation of dispersion stability of a colloidal suspension, and any physical change in colloidal suspension can be directly measured through electrical conductivity (Chereches and Minea 2019; Minea 2019). Generally, high electrical conductivity indicates the uniformity of NPs within the nanofluid which communicates the charges easily and shows good transportation of charges while

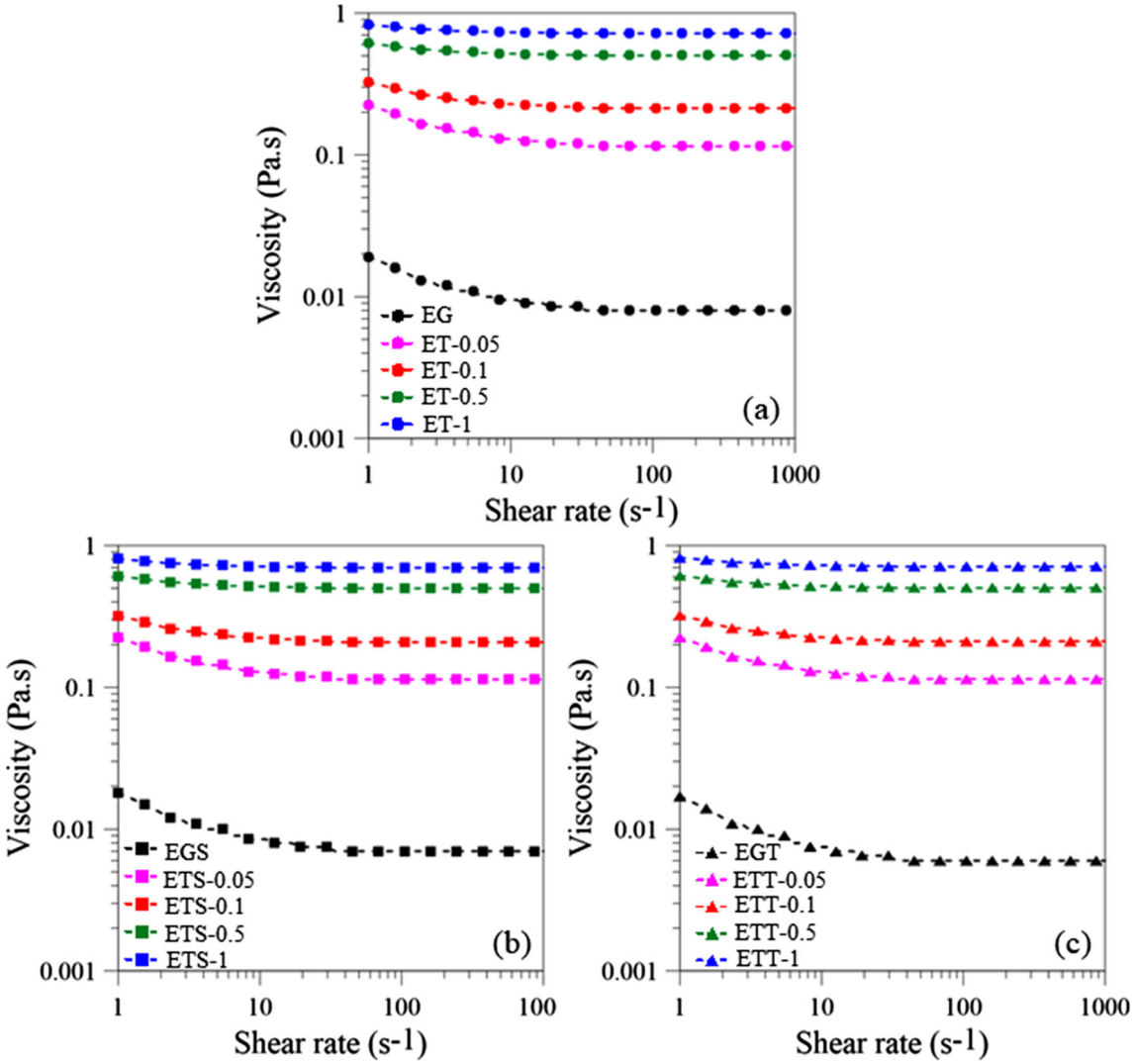

Fig. 6 Viscosity results showing shear-thinning behavior of nanofluids with varying shear rate (1–1000 s^{-1}) at ambient conditions: **a** EG, EG-titania nanofluids, **b** nanofluids with anionic surfactant SDS, **c** nanofluids with nonionic surfactant TX-100

low electrical conductivity is a representation of less population of NPs within the nanofluid or agglomeration of NPs within the nanofluid. Therefore, the change in the physical structure of nanofluid can be easily identified using electrical conductivity measurements. The electrical conductivity measurements for formulated nanofluids were carried out up to 2 wt% at room temperature and high temperature. The electrical conductivity was measured 3.7 μS/cm for EG solution while it increased to 35 μS/cm for ET-0.05 nanofluid as shown in Fig. 4. The reason for the sudden increase in electrical conductivity is attributed to the inclusion of titania nanofluid. In addition to this, a further increase in electrical conductivity was observed with an increase in TiO_2 NPs concentration in the solution. Generally, a uniform population of NPs ensures better charge dispersion and thus, the electrical conductivity showed higher values for ET-0.1, ET-0.5, and ET-1.0 nanofluid and was measured as 43, 57, 66 μS/cm, respectively (Fig. 4). The increased values of electrical conductivity are a good sign of the uniform distribution of NPs and higher surface potential. Furthermore, improvement in electrical conductivity was measured after the inclusion of surfactant and the values reached 5.2, 47, 578, 67, and 78 μS/cm for EGS, ETS-0.05, ETS-0.1, ETS-0.5, and ETS-1.0 nanofluid, respectively and 4.5, 42, 55, 64, and 75 μS/cm for EGT, ETT-0.05, ETT-0.1, ETT-0.5, and ETT-1.0 nanofluids, respectively (Fig. 4). The reason for higher electrical conductivity is credited to the surfactant micelles which can generally increase the surface charge of NPs as it was measured as zeta potential in DLS results (Fig. 2). In addition, the obtained results were performed up to 2 wt% of TiO_2 and found very few changes in zeta potential value.

Moreover, it was seen that temperature also has a significant effect on nanofluid stability. With an increase in temperature further increase in electrical conductivity was observed (Fig. 5). Figure 5a represents electrical conductivity results for ET nanofluids (without surfactants). In addition to this, the change in electrical conductivity is less at higher concentrations of nanofluid and the electrical conductivity values become stable at a higher temperature (80–90 °C) also shown in Table 3. A similar effect was also observed after the

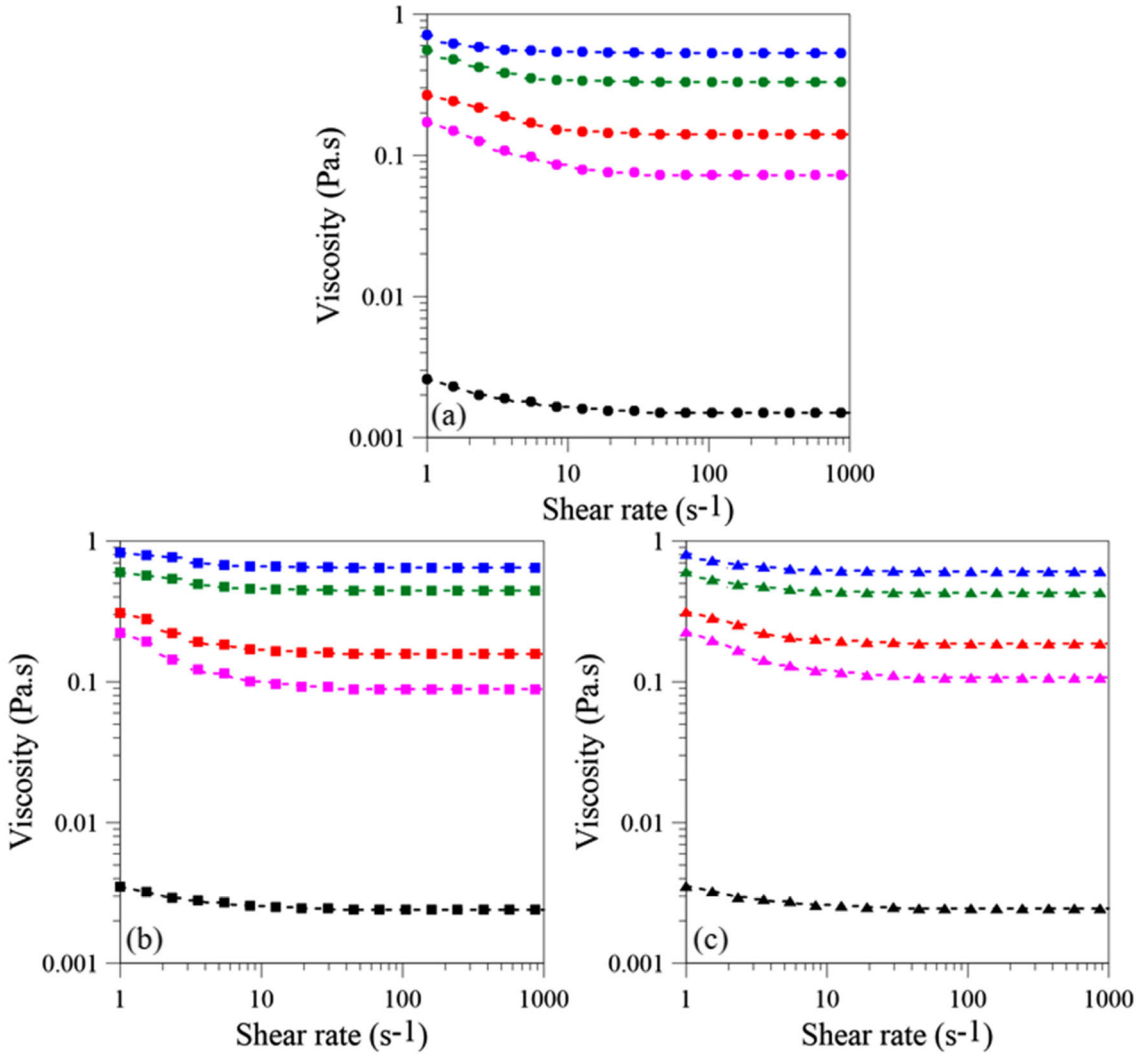

Fig. 7 Variation in viscosity with varying shear rate for nanofluids (**a**) without surfactant (**b**) with SDS (c) TX-100; at higher temperature 90 °C

addition of surfactant SDS and TX-100 surfactant in the nanofluid (Fig. 5b and c). Therefore, these particles acquire a random motion within the nanofluid and show improvement in electrical conductivity. These results depict that the TiO_2 nanofluid is very stable over a wide range of temperatures. Also, the inclusion of the surfactant maintains the uniform distribution of NPs within the nanofluid by improving the surface potential of NPs in the nanofluid. Thus, it can be said that this nanofluid exhibits characteristics for potential industrial applications. These results also highlight the fact that the role of surfactant as a stabilizer is very important along with NPs.

Viscosity results of EG-TiO_2 nanofluid

Nanofluid stability can be also supported by viscosity analysis as a part of the rheological investigation, which is an effective method to understand the nanofluid flow behavior for several industrial applications (Kamibayashi et al. 2006; Wei et al. 2016; Vázquez-Quesada et al. 2016). Therefore, the viscosity measurements were performed at varying shear rates 1–1000 s^{-1} and are shown in Fig. 6. The viscosity of the EG solution was determined 0.019 Pa s at a shear rate of 1 s^{-1} which is similar to the reported value by Sun and Teja (2003). Furthermore, a reduction in viscosity values was found with an increase in shear rate which showed shear-thinning behavior of non-Newtonian fluid (Fig. 6a). Moreover, the viscosity values increased after addition of TiO_2 NPs and reached to 0.225, 0.323, 0.611, and 0.826 Pa s for ET-0.05, ET-0.1, ET-0.5, and ET-1.0, respectively. All the formulations depicted viscosity reduction with the shear rate which is typical shear-thinning behavior for a nanofluid (Fig. 6a). However, after the inclusion of the surfactant in the nanofluid, a slight reduction in viscosity values was obtained at 1 s^{-1} shear rate due to interfacial tension reduction between the rheometer part (bob) and surfactant added nanofluid. Generally, resistance to flow is defined as viscosity, and after the addition of surfactant SDS, the resistance measured by the instrument is slightly lower than the measured in nanofluid without surfactant (Fig. 6b and c). The viscosity values were measured 0.018, 0.224, 0.318, 0.607, and 0.806 Pa s for EGS, ETS-0.05, ETS-0.1, ETS-0.5, and ETS-1.0, respectively. A similar effect was also observed in the case of TX-100 nanofluids and these values were found 0.018, 0.223, 0.321, 0.613, and 0.821 Pa s for EGT, ETT-0.05, ETT-0.1, ETT-0.5, and ETT-1.0, respectively.

Furthermore, the effect of high temperature (90 °C) on viscosity was also performed and results are shown in Fig. 7. An increase in temperature has a severe effect on the viscosity of EG, and the viscosity for EG was obtained at 0.0026 Pa s while it was found higher for ET-0.05 (0.172 Pa s) nanofluid (Fig. 7a). Similarly, the viscosities were obtained 0.247, 0.554, and 0.72 Pa s for ET-0.1, ET-0.5, and ET-1.0 nanofluid. Generally, EG-based nanofluid viscosity reduces with an increase in temperature due to thermal degradation (Islam and Shabani 2019). From the results, it is very clear that the inclusion of TiO_2 NPs can not only enhance the viscosity of base fluid but it can also provide a sustainable viscosity profile at high temperatures. And, this thermal property

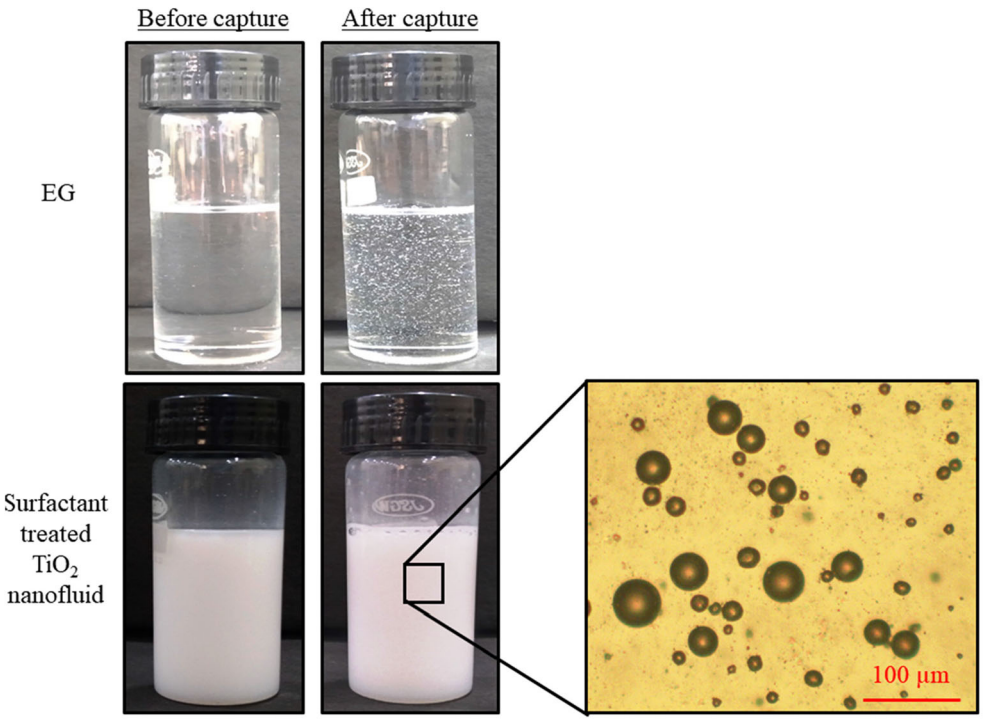

Fig. 8 Visual and microscopic appearance of TiO_2 nanofluid (with and without surfactant treated) before and after CO_2 capture

of TiO_2 makes the nanofluid suitable for several industrial applications where the previously high temperature was a limiting factor. Moreover, the inclusion of surfactant provides uniform distribution of NPs within the nanofluid which has a significant impact on rheological properties at high temperatures. The viscosity values were observed 0.0035, 0.22, 0.307, 0.597, and 0.79 Pa s for EGS, ETS-0.05, ETS-0.1, ETS-0.5, and ETS-1.0 nanofluid, respectively (Fig. 7b). Similarly, the values observed were 0.0033, 0.21, 0.29, 0.57, and 0.78 Pa s for EGT, ETT-0.05, ETT-0.1, ETT-0.5, and ETT-1.0 nanofluid, respectively (Fig. 7c). Now, it is very clear from the results that uniform distribution of NPs can be maintained using surfactant which can further provide thermal stability to the TiO_2 nanofluid for high-temperature applications where the conventional fluid is not applicable.

CO_2 capturing potential of titania nanofluids

Finally, the CO_2 capturing the potential of the titania nanofluids was evaluated under varying confining pressure and temperature and visual images are shown in Fig. 8 at ambient conditions. The CO_2 capturing in EG and EG-based titania nanofluid (0.5 wt%) is proved which illustrate the enhanced capturing capability in case of titania nanofluid. Furthermore, a microscopic study of CO_2 captured nanofluid is taken which shows the captured bubbles within the nanofluid. Two nanofluid concentrations (0.1 and 1 wt%) were explored in this study. Given the usual composition of flue gas emitted from a power plant are 8–10 vol.% H_2O, 3–5 vol.% O_2, 12–14 vol.% CO_2, and 72–77 vol.% N_2; in this study, a synthetic flue gas comprising of 20 vol.% CO_2 and 80 vol.% N_2 was formulated by mixing the gases for

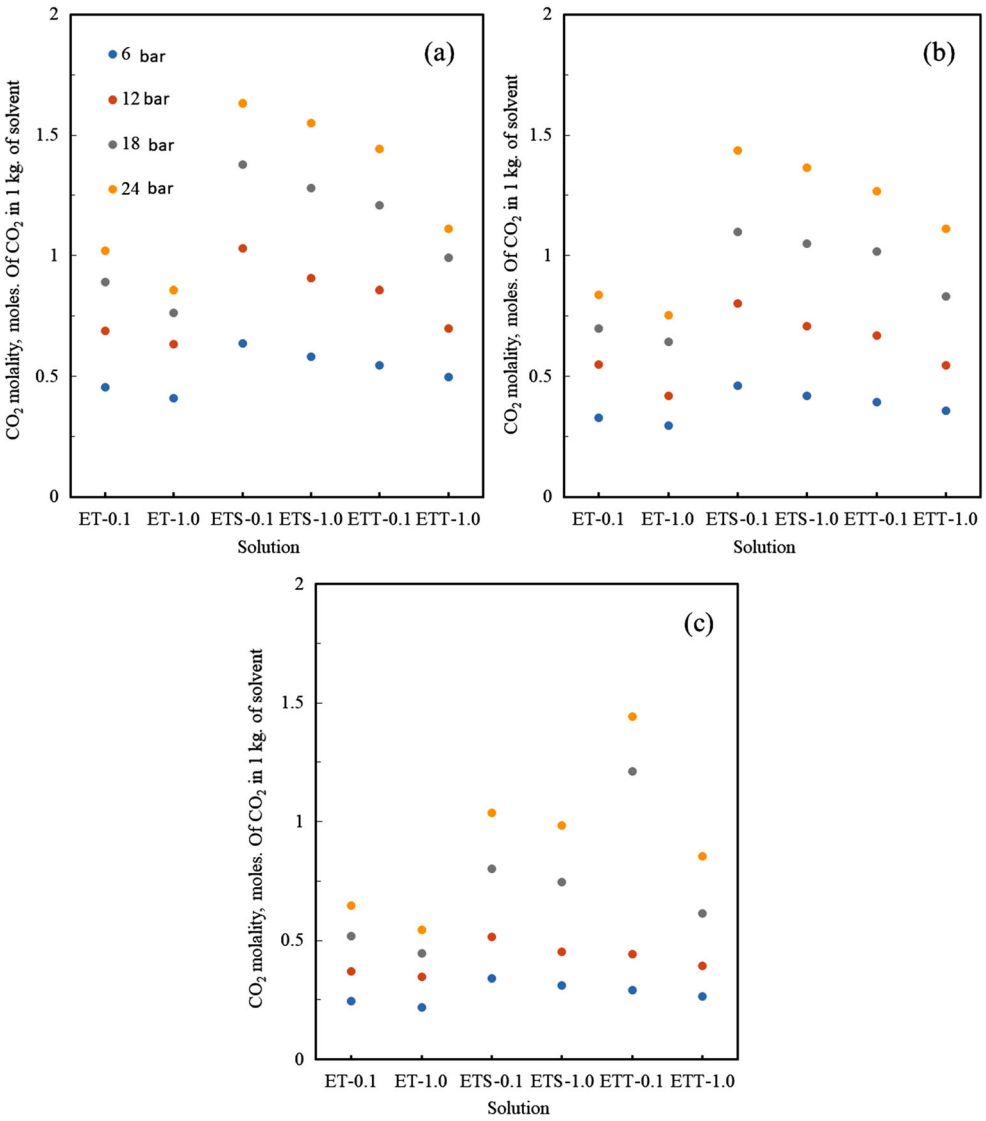

Fig. 9 CO_2 molality in different titania nanofluids at varying confining pressures (6–24 bar). The experiments were performed at **a** 30 °C, **b** 60 °C, and **c** 90 °C

absorption study (Kang and Lee 2000). Using flue gas instead of pure CO_2 also has the advantage of reducing the cost to purify CO_2 and in absence of any industrial applications which would extract monetary benefit from its separation, injecting CO_2 (or flue gas)-saturated nanofluid to the subsurface would be highly viable for its effective sequestration. Thus, the CO_2 loading potential of the nanofluids was explored at varying temperatures (30 and 90 °C) and confining pressure (6–24 bar) using the well-established pressure decay method (Haghtalab et al. 2015; Haider et al. 2018; Chaturvedi and Sharma 2020). The agitation was provided by the impeller rotating at a speed of 600. The CO_2 absorption of the nanofluids has been reported in form of CO_2 molality which is the measure of no. of moles of CO_2 absorbed inside a kilogram of the solvent. These observations have been presented in Fig. 9. Initially, the titania nanofluids (without any surfactant) were evaluated in the stirring pot. They exhibited a molality of 0.46 mol/kg of solvent and 0.4 mol/kg of solvent at a confining pressure of 6 bar and temperature of 30 °C for NP concentrations 0.1 and 1 wt%, respectively (Fig. 9a). The fall in gas loading at higher concentrations can be attributed to the agglomeration in nanofluids (check Fig. 1) which reduces NP surface area and thus their ability to participate in gas capture. Similarly, in nanofluids with lower particle size (thus higher surface area), more gas loading was observed, even at lower pressures, with maximum CO_2 loading observed in ETS 0.1 nanofluid (0.638 mol/kg of solvent, 6 bar, 30 °C) (Fig. 9a). Increasing pressure increased CO_2 absorption in all solutions with maximum CO_2 loading (1.63 mol/kg of solvent) observed in ETS-0.1 at 24 bars (Fig. 9a). The positive influence of pressure has already been documented in past literature and increasing the confining pressure brings more CO_2 (or flue gas) in contact with the nanofluid interface, which ultimately increases gas entrapment (Haghtalab et al. 2015; Chaturvedi et al. 2018). Increasing the temperature caused a decrease (≈ 30%, Fig. 9b, c) in the values of gas loading at lower pressure ranges which can be attributed to the increased kinetic movement of gas molecules at high temperature that causes instability in gas bubbles and destabilize them before their entrapment. However, on increasing pressure, the destabilizing role of temperature on CO_2 is negated and at higher pressures (> 18 bar), only a 16–20% fall in CO_2 loading was observed. Thus, for the high-temperature capture of CO_2 from the thermal power plant exhaust, higher pressure should be recommended.

Finally, the role of agitation speed (RPM of the impeller) was studied on the gas absorption of the titania nanofluids. The RPM was varied for 300–1800 for SDS-treated nanofluids (ETS-0.1 and ETS-1.0) and these observations have been reported in Fig. 10. At a lower agitation rate (≈ 300), the CO_2 molality was inferior as less agitation leads to

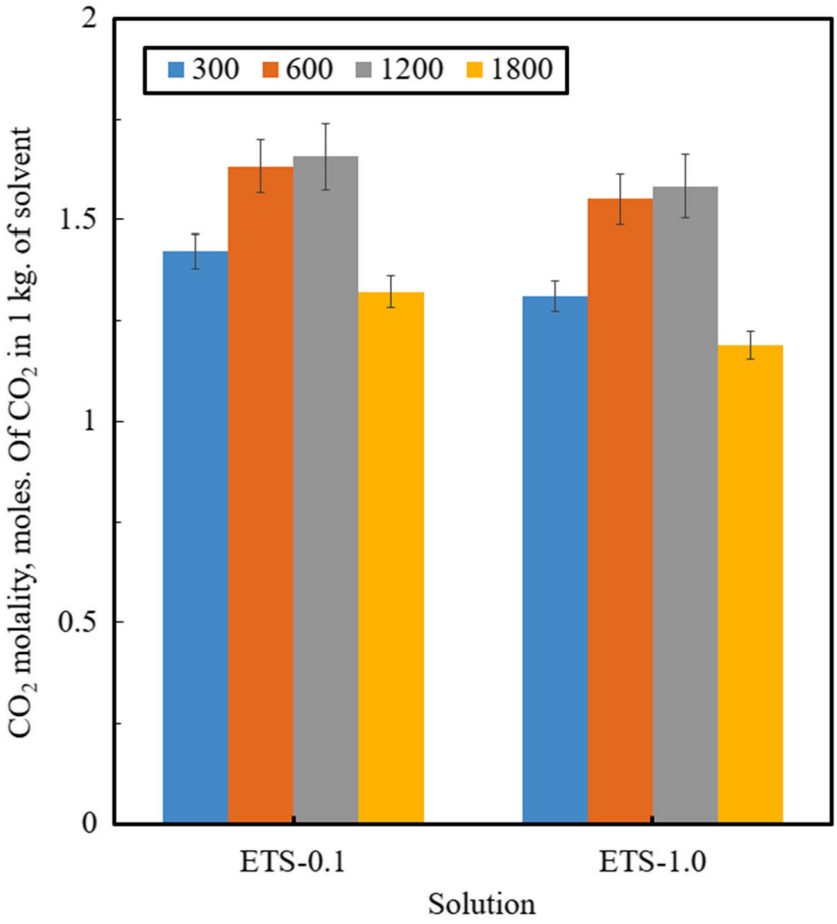

Fig. 10 CO_2 molality in SDS-treated titania nanofluids at varying agitation rates (300–1800 rpm). The investigations were performed at 30 °C and 24 bar

a drop in gas bubbles entering the nanofluid for entrapment. Similar values of gas molality were observed for both, RPM 600 and 1200, indicating that gas molality is influenced by moderate RPM values as the agitation is adequate to ensure that most of the gas bubbles can enter the solution to be physically entrapped in the interstitial space between the liquid layers. However, at higher RPM values, low gas absorption is observed because higher RPM causes too much instability in the system (similar to the increase in gas kinetic energy on increasing temperature); thus, lower values of gas absorption are observed (Chaturvedi et al. 2018; Chaturvedi et al. 2020) This proves that the design of nanofluid-CO_2 gas absorption systems requires careful design and optimization. The observations indicate that titania nanofluids with SDS treatment can be effective in the role of carbon capture and storage. This work is fully dedicated to the thermal and physical stability of surfactant-treated nanofluids for CO_2 capture followed by understanding the rheological characterization of nanofluids after and before CO_2 capture. This work also highlights the potential application of CO_2 captured fluid in oil recovery projects and simultaneous CO_2 storage in subsurface applications which may be beneficial for reducing carbon footprint from the environments.

Conclusions

In this study, TiO_2 nanofluid was prepared in the base solution of ethylene glycol (EG) with and without surfactant, and results were analyzed using dynamic light scattering (DLS) study, electrical conductivity, and viscosity measurement at 30 and 90 °C. The TiO_2 nanofluid showed high dispersion stability and lesser agglomeration as reported in the literature, and the size was measured 280 nm for ET-0.05 (0.05 wt% of TiO_2), while it increased to 409 nm (ET-1.0) with an increase in the concentration of TiO_2 NPs in a nanofluid. However, the agglomeration of NPs can be controlled via the inclusion of surfactant; thus, anionic surfactant (SDS) and nonionic surfactant (TX-100) were added in the nanofluid which resulted in the reduction of NP agglomeration and the size reached 217 and 229 nm for ETS-0.05 and ETT-0.05 and 249 and 298 nm for ETS-1.0 and ETT-1.0, respectively. The reason for the reduced size of NPs clusters is credited to the inclusion of anionic surfactants, which forms micelles in the nanofluid and gets adsorbed on the interface of NPs, resulting in enhanced surface potential of NPs. Similar to that, nonionic surfactant increases the zeta potential via surface laying mechanism which help to curtail the attractive forces and increases the zeta potential. Thus, the zeta potential values increased after the inclusion of surfactants in the nanofluid (DLS study) from − 40 to − 53 mV (SDS added titania nanofluid ETS-1.0) and − 49.5 mV for (Tx-100 added titania nanofluid ETS-1.0). Furthermore, nanofluid stability was examined at high temperatures using electrical conductivity and the results showed that the higher dispersion stability of nanofluids can be obtained using an anionic and nonionic surfactant. Furthermore, viscosity measurement of EG was found inefficient at higher temperatures as compared to the viscosity results at ambient conditions, which can be further improved using the addition of TiO_2. Additionally, the inclusion of surfactant has shown promising results at higher temperatures due to the uniform distribution of NPs within the nanofluid which govern the matter at the nano-scale level and helped the nanofluid to maintain the rheological stability for potential use in high-temperature industrial applications. Finally, the SDS-treated titania nanofluids showed strong CO_2 capturing ability with CO_2 loading found to be positively influenced by increasing pressure and rate of agitation at 30 °C (0.4 mol/kg of solvent at 6 bar to 1.63 mol/kg of solvent at 24 bar) while increasing the temperature reduced CO_2 loading. Thus, this study suggests that the optimized condition for CO_2 capture is high pressure and low temperature (pressure > 18 bar and temperature less than ambient). Based on the observations of this study, the application of anionic surfactant-treated titania nanofluids is recommended for CO_2 capture and storage applications and also can be useful for oil recovery applications.

Acknowledgements The authors would like to acknowledge the EOR Laboratory research group and Rajiv Gandhi Institute of Petroleum Technology for the infrastructural and funding support.

Author contributions Ravi Shankar Kumar: conceptualization, methodology, writing—original draft preparation. Rishiraj Goswami: data curation. Krishna Raghav Chaturvedi: visualization, investigation. Tushar Sharma: supervision, validation, writing—reviewing and editing, project administration.

Data availability The authors will make available the data and associated protocols promptly available to readers without undue qualifications.

Declarations

Ethical approval Not applicable.

Consent to participate and publish All authors confirm their participation in this study, have read the final manuscript, and have given their consent for the publication of this study.

Competing interests The authors declare no competing interests.

References

Ahmed A, Mohd Saaid I, Pilus MR et al (2018) Development of surface treated nanosilica for wettability alteration and interfacial tension reduction. J Dispers Sci Technol 39:1469–1475

Al Mesfer MK (2020) Synthesis and characterization of high-performance activated carbon from walnut shell biomass for CO_2 capture. Environ Sci Pollut Res 27:15020–15028

Al-Anssari S, Arif M, Wang S et al (2017) Stabilising nanofluids in saline environments. J Colloid Interface Sci 508:222–229

Al-Waeli AHA, Chaichan MT, Kazem HA, Sopian K (2019) Evaluation and analysis of nanofluid and surfactant impact on photovoltaic-thermal systems. Case Stud Therm Eng 13:100392

Asadi-Sangachini Z, Galangash MM, Younesi H, Nowrouzi M (2019) The feasibility of cost-effective manufacturing activated carbon derived from walnut shells for large-scale CO_2 capture. Environ Sci Pollut Res 26:26542–26552

Azzolina NA, Peck WD, Hamling JA, Gorecki CD, Ayash SC, Doll TE, Nakles DV, Melzer LS (2016) How green is my oil? A detailed look at greenhouse gas accounting for CO_2-enhanced oil recovery (CO_2-EOR) sites. Int J Greenh Gas Control 51:369–379

Borhani TN, Wang M (2019) Role of solvents in CO_2 capture processes: the review of selection and design methods. Renew Sust Energ Rev 114:109299 9

Chaturvedi KR, Kumar R, Trivedi J et al (2018) Stable silica nanofluids of an oilfield polymer for enhanced CO_2 absorption for oilfield applications. Energy Fuel 32:12730–12741

Chaturvedi KR, Narukulla R, Amani M, Sharma T (2021) Experimental investigations to evaluate surfactant role on absorption capacity of nanofluid for CO_2 utilization in sustainable crude mobilization. Energy 225:120321

Chaturvedi KR, Sharma T (2020) Carbonated polymeric nanofluids for enhanced oil recovery from sandstone reservoir. J Pet Sci Eng 194: 107499. https://doi.org/10.1016/j.petrol.2020.107499

Chaturvedi KR, Sharma T (2021) Rheological analysis and EOR potential of surfactant treated single-step silica nanofluid at high temperature and salinity. J Pet Sci Eng 196:107704

Chaturvedi KR, Trivedi J, Sharma T (2020) Single-step silica nanofluid for improved carbon dioxide flow and reduced formation damage in porous media for carbon utilization. Energy 197:117276

Chen H, Ding Y, He Y, Tan C (2007) Rheological behaviour of ethylene glycol based titania nanofluids. Chem Phys Lett 444:333–337

Chereches EI, Minea AA (2019) Electrical conductivity of new nanoparticle enhanced fluids: an experimental study. Nanomaterials 9:1228

Demir H, Dalkilic AS, Kürekci NA, Duangthongsuk W, Wongwises S (2011) Numerical investigation on the single phase forced convection heat transfer characteristics of TiO_2 nanofluids in a double-tube counter flow heat exchanger. Int Commun Heat Mass Transf 38: 218–228

Ding G, Peng H, Jiang W, Gao Y (2009) The migration characteristics of nanoparticles in the pool boiling process of nanorefrigerant and nanorefrigerant-oil mixture. Int J Refrig 32:114–123

Esfandyari Bayat A, Junin R, Samsuri A et al (2014) Impact of metal oxide nanoparticles on enhanced oil recovery from limestone media at several temperatures. Energy Fuel 28:6255–6266 6

Grassian VH, O'Shaughnessy PT, Adamcakova-Dodd A, Pettibone JM, Thorne PS (2007) Inhalation exposure study of titanium dioxide nanoparticles with a primary particle size of 2 to 5 nm. Environ Health Perspect 115:397–402

Haddad Z, Abid C, Oztop HF, Mataoui A (2014) A review on how the researchers prepare their nanofluids. Int J Therm Sci 76:168–189

Haghtalab A, Mohammadi M, Fakhroueian Z (2015) Absorption and solubility measurement of CO_2 in water-based ZnO and SiO_2 nanofluids. Fluid Phase Equilib 392:33–42

Haider MB, Jha D, Marriyappan Sivagnanam B, Kumar R (2018) Thermodynamic and kinetic studies of CO_2 capture by glycol and amine-based deep eutectic solvents. J Chem Eng Data 63:2671–2680

Huminic G, Huminic A (2012) Application of nanofluids in heat exchangers: a review. Renew Sust Energ Rev 16:5625–5638

Islam R, Shabani B (2019) Prediction of electrical conductivity of TiO_2 water and ethylene glycol-based nanofluids for cooling application in low temperature PEM fuel cells. In: Energy Procedia. Elsevier Ltd, pp 550–557

Jain P, Pathak K, Tripathy S (2013) Possible source-sink matching for CO_2 sequestration in Eastern India. In: Energy Procedia. Elsevier Ltd, pp 3233–3241

Jiang L, Li S, Yu W, Wang J, Sun Q, Li Z (2016) Interfacial study on the interaction between hydrophobic nanoparticles and ionic surfactants. Colloids Surf A Physicochem Eng Asp 488:20–27

Jiang JZ, Zhang S, Fu XL, Liu L, Sun BM (2019) Review of gas–liquid mass transfer enhancement by nanoparticles from macro to microscopic. Heat Mass Transf Stoffuebertragung 55:2061–2072

Jiang J, Zhao B, Zhuo Y, Wang S (2014) Experimental study of CO_2 absorption in aqueous MEA and MDEA solutions enhanced by nanoparticles. Int J Greenh Gas Control 29:135–141

Kamibayashi M, Ogura H, Otsubo Y (2006) Rheological behavior of suspensions of silica nanoparticles in associating polymer solutions. Ind Eng Chem Res 45:6899–6905

Kang SP, Lee H (2000) Recovery of CO_2 from flue gas using gas hydrate: thermodynamic verification through phase equilibrium measurements. Environ Sci Technol 34:4397–4400

Krishnan A, Gopinath KP, Vo DVN, Malolan R, Nagarajan VM, Arun J (2020) Ionic liquids, deep eutectic solvents and liquid polymers as green solvents in carbon capture technologies: a review. Environ Chem Lett 18:2031–2054

Kumar RS, Chaturvedi KR, Iglauer S, Trivedi J, Sharma T (2020) Impact of anionic surfactant on stability, viscoelastic moduli, and oil recovery of silica nanofluid in saline environment. J Pet Sci Eng 195: 107634

Kumar RS, Narukulla R, Sharma T (2020) Comparative effectiveness of thermal stability and rheological properties of nanofluid of SiO_2-TiO_2 nanocomposites for oil field applications. Ind Eng Chem Res 59:15768–15783

Kumar RS, Sharma T (2018) Stability and rheological properties of nanofluids stabilized by SiO_2 nanoparticles and SiO_2-TiO_2 nanocomposites for oilfield applications. Colloids Surf A Physicochem Eng Asp 539:171–183

Kumar RS, Sharma T (2020) Stable SiO_2 –TiO_2 composite-based nanofluid of improved rheological behaviour for high-temperature oilfield applications. Geosystem Eng 1–11

Lam S, Velikov KP, Velev OD (2014) Pickering stabilization of foams and emulsions with particles of biological origin. Curr Opin Colloid Interface Sci 19:490–500

Leung DYC, Caramanna G, Maroto-Valer MM (2014) An overview of current status of carbon dioxide capture and storage technologies. Renew Sust Energ Rev 39:426–443

Liu J, Xie L, Yao Y, Gan Q, Zhao P, du L (2019) Preliminary study of influence factors and estimation model of the enhanced gas recovery stimulated by carbon dioxide utilization in shale. ACS Sustain Chem Eng 7:20114–20125

Minea AA (2019) A review on electrical conductivity of nanoparticle-enhanced fluids. Nanomaterials 9:1592

Nashed O, Partoon B, Lal B, Sabil KM, Shariff AM (2018) Review the impact of nanoparticles on the thermodynamics and kinetics of gas hydrate formation. J Nat Gas Sci Eng 55:452–465

Palabiyik I, Musina Z, Witharana S, Ding Y (2011) Dispersion stability and thermal conductivity of propylene glycol-based nanofluids. J Nanopart Res 13:5049–5055

Peyghambarzadeh SM, Hashemabadi SH, Hoseini SM, Seifi Jamnani M (2011) Experimental study of heat transfer enhancement using water/ethylene glycol based nanofluids as a new coolant for car radiators. Int Commun Heat Mass Transf 38:1283–1290

Peyravi A, Keshavarz P, Mowla D (2015) Experimental investigation on the absorption enhancement of CO2 by various nanofluids in hollow fiber membrane contactors. Energy Fuel 29:8135–8142

Pilorgé H, McQueen N, Maynard D, Psarras P, He J, Rufael T, Wilcox J (2020) Cost analysis of carbon capture and sequestration of process emissions from the U.S. Industrial Sector. Environ Sci Technol 54: 7524–7532

Rafati R, Smith SR, Sharifi Haddad A, Novara R, Hamidi H (2018) Effect of nanoparticles on the modifications of drilling fluids properties: a review of recent advances. J Pet Sci Eng 161:61–76

Rezakazemi M, Darabi M, Soroush E, Mesbah M (2019) CO_2 absorption enhancement by water-based nanofluids of CNT and SiO_2 using hollow-fiber membrane contactor. Sep Purif Technol 210:920–926

Saidur R, Leong KY, Mohammad HA (2011) A review on applications and challenges of nanofluids. Renew Sust Energ Rev 15:1646–1668

Satti JR, Das DK, Ray D (2017) Investigation of the thermal conductivity of propylene glycol nanofluids and comparison with correlations. Int J Heat Mass Transf 107:871–881

Schrag DP (2007) Preparing to capture carbon. Science (80) 315:812–813

Sekrani G, Poncet S (2018) Ethylene- and propylene-glycol based nanofluids: a litterature review on their thermophysical properties and thermal performances. Appl Sci 8:2311

Setia H, Gupta R, Wanchoo RK (2013) Stability of nanofluids. Mater Sci Forum 757:139–149

Sun T, Teja AS (2003) Density, viscosity, and thermal conductivity of aqueous ethylene, diethylene, and triethylene glycol mixtures between 290 K and 450 K. J Chem Eng Data 48:198–202

Thakkar A, Raval A, Chandra S et al (2019) A comprehensive review of the application of nano-silica in oil well cementing. Petroleum 6: 123–129

Tiwari AK, Ghosh P, Sarkar J (2013) Heat transfer and pressure drop characteristics of CeO_2/water nanofluid in plate heat exchanger. Appl Therm Eng 57:24–32

Tolesorkhi SF, Esmaeilzadeh F, Riazi M (2018) Experimental and theoretical investigation of CO_2 mass transfer enhancement of silica nanoparticles in water. Pet Res 3:370–380

Torres Pineda I, Lee JW, Jung I, Kang YT (2012) CO_2 absorption enhancement by methanol-based Al_2O_3 and SiO_2 nanofluids in a tray column absorber. Int J Refrig 35:1402–1409

Vázquez-Quesada A, Tanner RI, Ellero M (2016) Shear thinning of noncolloidal suspensions. Phys Rev Lett 117:108001

Vega F, Sanna A, Navarrete B, Maroto-Valer MM, Cortés VJ (2014) Degradation of amine-based solvents in CO_2 capture process by chemical absorption. Greenh Gases Sci Technol 4:707–733

Wang T, Yu W, Liu F, Fang M, Farooq M, Luo Z (2016) Enhanced CO_2 absorption and desorption by monoethanolamine (MEA)-based nanoparticle suspensions. Ind Eng Chem Res 55:7830–7838

Wei B, Li Q, Jin F, Li H, Wang C (2016) The potential of a novel nanofluid in enhancing oil recovery. Energy Fuel 30:2882–2891

William JKM, Ponmani S, Samuel R, Nagarajan R, Sangwai JS (2014) Effect of CuO and ZnO nanofluids in xanthan gum on thermal, electrical and high pressure rheology of water-based drilling fluids. J Pet Sci Eng 117:15–27

Xie H, Yu W, Chen W (2010) MgO nanofluids: higher thermal conductivity and lower viscosity among ethylene glycol-based nanofluids containing oxide nanoparticles. J Exp Nanosci 5:463–472

Yuan B, Wang W (2018) Using nanofluids to control fines migration for oil recovery: nanofluids co-injection or nanofluids pre-flush? -A comprehensive answer. Fuel 215:474–483

Zare P, Keshavarz P, Mowla D (2019) Membrane absorption coupling process for CO_2 capture: application of water-based ZnO, TiO_2, and multi-walled carbon nanotube nanofluids. Energy Fuel 33:1392–1403

Zhang Z, Cai J, Chen F, Li H, Zhang W, Qi W (2018) Progress in enhancement of CO2 absorption by nanofluids: a mini review of mechanisms and current status. Renew Energy 118:527–535